

## Supporting Information

### **Topochemical cross-linking of diacetylene in a highly interpenetrated three-dimensional covalent organic framework**

Shangqing Liu,<sup>ac</sup> Mengyao Chen,<sup>ac</sup> Yu Zhao,<sup>\*ac</sup> Guolong Xing,<sup>ac</sup> Weidong Zhu<sup>ac</sup> and Teng Ben<sup>\*abc</sup>

<sup>a</sup>Zhejiang Engineering Laboratory for Green Syntheses and Applications of Fluorine-Containing Specialty Chemicals, Institute of Advanced Fluorine-Containing Materials, Zhejiang Normal University, Jinhua 321004, P. R. China.

<sup>b</sup>Science and Technology Center for Quantum Biology, National Institute of Extremely-Weak Magnetic Field Infrastructure, Hangzhou 310000, P. R. China.

<sup>c</sup>Key Laboratory of the Ministry of Education for Advanced Catalysis Materials, Institute of Physical Chemistry, Zhejiang Normal University, Jinhua 321004, P. R. China.

*E-mail: zhaoyu@zjnu.edu.cn; tengben@zjnu.edu.cn*

## Contents

Section S1. Materials and Characterizations .....	3
Section S2. Synthetic Procedures .....	5
Section S3. Fourier-transform infrared spectroscopy.....	8
Section S4. Solid-state <sup>13</sup> C NMR spectra .....	9
Section S5. SEM image.....	10
Section S6. TEM imag.....	11
Section S7. TGA curves .....	12
Section S8. PXRD patterns and structures .....	13
Section S9. EDS analysis .....	15
Section S10. Raman spectroscopy analysis.....	16
Section S11. UV–visible absorption spectra.....	17
Section S12. Nitrogen adsorption .....	18
Section S13. Iodine uptake experiments .....	19
Section S14. Electrical conductivity measurements .....	20
Section S15. Fractional atomic coordinates.....	21
Section S16. References.....	23

## Section S1. Materials and Characterizations

### S1.1. Materials

All materials were reagent grade and used as received, unless stated otherwise. Tetrakis(4-bromophenyl)methane (Bide Pharmatech Co., Ltd., 95%), 4-aminophenylboronic acid pinacol ester (J&K scientific LTD, 98.0%), toluene (Sinopharm chemical reagent Co., Ltd.,  $\geq 99.5\%$ ), sodium hydroxide (Sinopharm chemical reagent Co., Ltd.,  $\geq 96.0\%$ ), dichlorobis(triphenylphosphine)palladium(II) (J&K scientific LTD, 98.0%), 4-ethynylbenzaldehyde (Aladdin<sup>®</sup>,  $\geq 98.0\%$ ), copper(II) acetate (J&K scientific LTD,  $\geq 98.0\%$ ), methanol (Sinopharm chemical reagent Co., Ltd.,  $\geq 99.7\%$ ), *n*-hexane (Sinopharm chemical reagent Co., Ltd.,  $\geq 97.0\%$ ), ethyl acetate (EA, Sinopharm chemical reagent Co., Ltd.,  $\geq 99.5\%$ ), 1,3,5-trimethylbenzene (Aladdin<sup>®</sup>,  $\geq 98.0\%$ ), acetic acid (Sinopharm chemical reagent Co., Ltd.,  $\geq 99.5\%$ ), concentrated hydrochloric acid (Sinopharm chemical reagent Co., Ltd., 36.0%-38.0%), iodine (J&K scientific LTD,  $\geq 99.8\%$ ), tetrahydrofuran (THF, Sinopharm chemical reagent Co., Ltd.,  $\geq 99.0\%$ ), dichloromethane (DCM, Sinopharm chemical reagent Co., Ltd.,  $\geq 99.5\%$ ), acetone (Sinopharm chemical reagent Co., Ltd.,  $\geq 99.5\%$ ), Na<sub>2</sub>SO<sub>4</sub> (Sinopharm chemical reagent Co., Ltd.,  $\geq 99.0\%$ ). The solvents were purified and dried according to the standard techniques: THF, methanol, 1,3,5-trimethylbenzene and pyridine was distilled from CaH<sub>2</sub>.

### S1.2. Characterizations

**Nuclear magnetic resonance (NMR) spectroscopy.** <sup>1</sup>H NMR spectra were measured on a Bruker Fourier 400 MHz spectrometer. Solid-state NMR spectra were recorded at ambient pressure on a Bruker Fourier 600 MHz spectrometer using a standard CP pulse sequence probe with 3.2 mm (outside diameter) zirconia rotors. Unless otherwise stated, all spectra were measured at ambient temperature. The chemical shift for <sup>1</sup>H-NMR spectra was reported in parts per million (ppm) and referenced to characteristic solvent signals of partly deuterated solvents: CDCl<sub>3</sub> at 7.26 ppm and DMSO-d<sub>6</sub> at 2.50 ppm. The spin multiplicity and corresponding signal patterns were abbreviated as follows: s = singlet, d = doublet, t = triplet, q = quartet, quint. = quintet, sext. = sextet, m = multiplet and br = broad signal. Coupling constants *J* were noted in Hz.

**Fourier transform infrared (FT-IR) spectroscopy.** The FT-IR spectra (KBr) were obtained using a SHIMADZU IRAffinity-1 Fourier transform infrared spectrophotometer. A SHIMADZU UV-2450 spectrophotometer was used for all absorbance measurements.

**Powder X-ray diffraction (PXRD) analysis.** Powder X-ray diffraction (PXRD) patterns were carried out in reflection mode on a Bruker D8 advance powder diffractometer with Cu K $\alpha$  ( $\lambda = 1.5418 \text{ \AA}$ ) line focused radiation at 40 kV and 40 mA from  $2^\theta = 3.0^\circ$  up to  $40^\circ$  with 0.020481 increment by Bragg-Brentano. The powdered sample was added to the glass and compacted for measurement.

**Thermogravimetric analysis (TGA).** Thermogravimetric analysis (TGA) was recorded on a SHIMADZU DTG-60 thermal analyzer under N<sub>2</sub>. The operational range of the instrument was from 30 °C to 800 °C at a heating rate of 10 °C min<sup>-1</sup> with N<sub>2</sub> flow rate of 30 mL min<sup>-1</sup>.

**Differential scanning calorimetry (DSC).** Differential scanning calorimetry (DSC) analyses were

carried out on TA DSC 250 thermal analysis system at a heating rate of 10 K min<sup>-1</sup> within a temperature range of 30-350 °C. Subsequently, it was cooled to 30 °C at 10 K min<sup>-1</sup> and then raised to 350 °C at 10 K min<sup>-1</sup>. The samples were pretreated at 120 °C under dynamic vacuum to fully remove solvents trapped in the pores.

**Nitrogen isotherm measurements.** Nitrogen sorption experiments were performed at 77 K up to 1 bar using a nanometric sorption analyzer. The adsorption-desorption isotherms of N<sub>2</sub> were obtained at 77 K using a PhysChem Instruments Ltd iPore 400 gas sorption analyzers. Before sorption analysis, the sample was evacuated at 100 °C for 12 h using a turbomolecular vacuum pump. Specific surface areas were calculated from nitrogen adsorption data by multipoint BET analysis. Nonlocal density functional theory (NL-DFT) was applied to analyze the N<sub>2</sub> isotherm based on the model of N<sub>2</sub>@77 K on carbon with cylindrical pores.

**Scanning electron microscopy (SEM).** Scanning electron microscopy (SEM) was performed on a Zeiss Gemini SEM 300 microscope instrument. Samples were prepared by dispersing the material onto conductive adhesive tapes attached to a flat aluminum sample holder and then coated with gold.

**Energy dispersive spectroscopy (EDS).** EDS analysis was performed on a Zeiss Gemini SEM 300 microscope instrument.

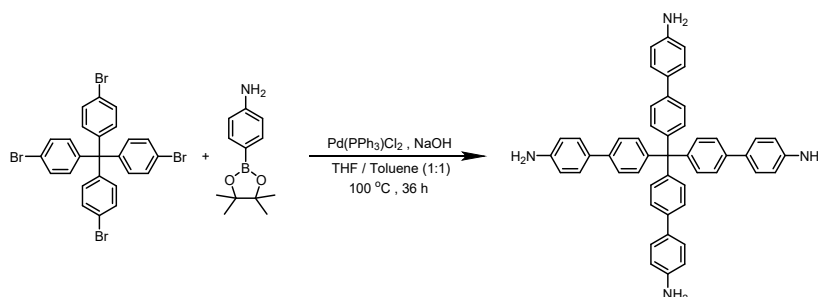
**Transmission electron microscope (TEM).** High resolution transmission electron microscope (HR-TEM) analysis was collected on a JEOL JEM-2100 microscope instrument at 200 kV. synthesized sample was dispersed into ethyl alcohol to obtain a highly dispersed suspension. Then, one droplet was transferred onto a carbon film supported TEM grid.

**Raman spectroscopy.** Raman spectra were obtained on LabRAM HR Evolution (HORIBA Scientific, Japan) equipped with an excitation source wavelength of 532 nm.

**UV-visible spectroscopy.** The UV-visible absorption spectra were recorded on a spectrophotometer (UV-2700, Shimadzu) utilizing BaSO<sub>4</sub> as the reference.

## Section S2. Synthetic Procedures

### Synthesis of tetrakis(4-amino biphenyl)methane (TABPM).



To a suspension of tetrakis(4-bromophenyl)methane (0.32 g, 0.50 mmol) and 4-aminophenylboronic acid pinacol ester (0.44 g, 2.0 mmol) in 14 mL of mixed solvent of tetrahydrofuran and toluene (1:1), sodium hydroxide (0.30 g, 7.5 mmol) was added, followed by the addition of PdCl<sub>2</sub>(PPh<sub>3</sub>)<sub>2</sub> (0.18 g, 0.25 mmol). The mixture was further degassed with nitrogen for three times and was refluxed at 100 °C for 36 h under nitrogen. THF and toluene were removed and methanol was added. After filtration, the filtrate sample was crystallized and dried under high vacuum for 10 h. Yield: 0.14 g, 41%. <sup>1</sup>H-NMR was in accordance with literature.<sup>1</sup>

<sup>1</sup>H-NMR (400 MHz, DMSO-*d*<sub>6</sub>): δ<sub>H</sub> [ppm] = 7.48 (d, J=8.5, 8H), 7.36 (d, J=8.5, 8H), 7.21 (d, J=8.5, 8H), 6.61 (d, J=8.5, 8H), 5.22 (s, 8H);

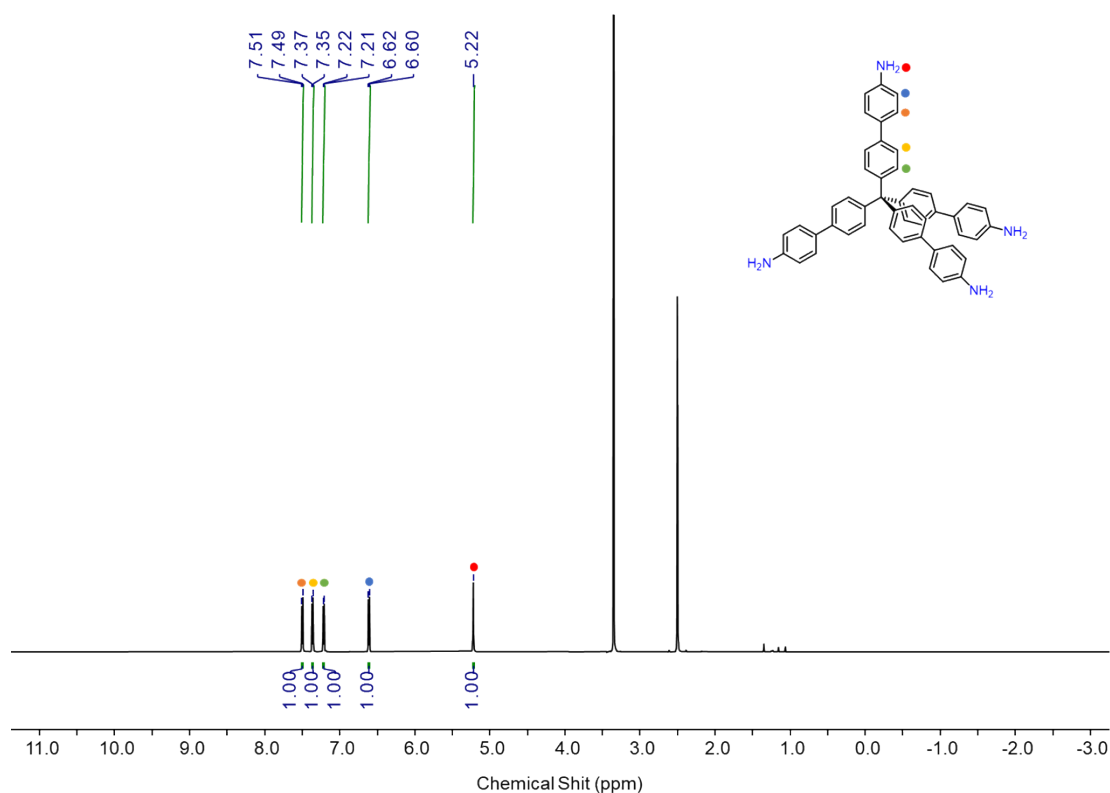
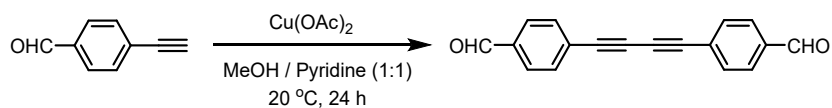


Fig. S1 The <sup>1</sup>H NMR spectra of tetrakis(4-amino biphenyl)methane in DMSO-*d*<sub>6</sub>.

**Synthesis of 4,4'-(buta-1,3-diyne-1,4-diyl)dibenzaldehyde (BDDA).**



Cu(OAc)<sub>2</sub> (2.7 g, 15.0 mmol, 2.50 eq.) was added to a solution of 4-ethynylbenzaldehyde (781 mg, 6.0 mmol) in pyridine/MeOH 1:1 (v/v; 60 ml). After the solution was stirred at 20 °C for 24 h, all volatiles were removed under reduced pressure, purification via column chromatography using EA/*n*-hexane [1:4] as eluent yielded the product as pale-yellow powder (450 mg, 1.74 mmol) in a yield of 58%. <sup>1</sup>H-NMR was in accordance with literature.<sup>2</sup>

<sup>1</sup>H-NMR (400 MHz, CDCl<sub>3</sub>): δ<sub>H</sub> [ppm] = 10.04 (s, 2H), 7.88 (d, *J* = 8.0 Hz, 4H), 7.69 (d, *J* = 8.0 Hz, 4H);

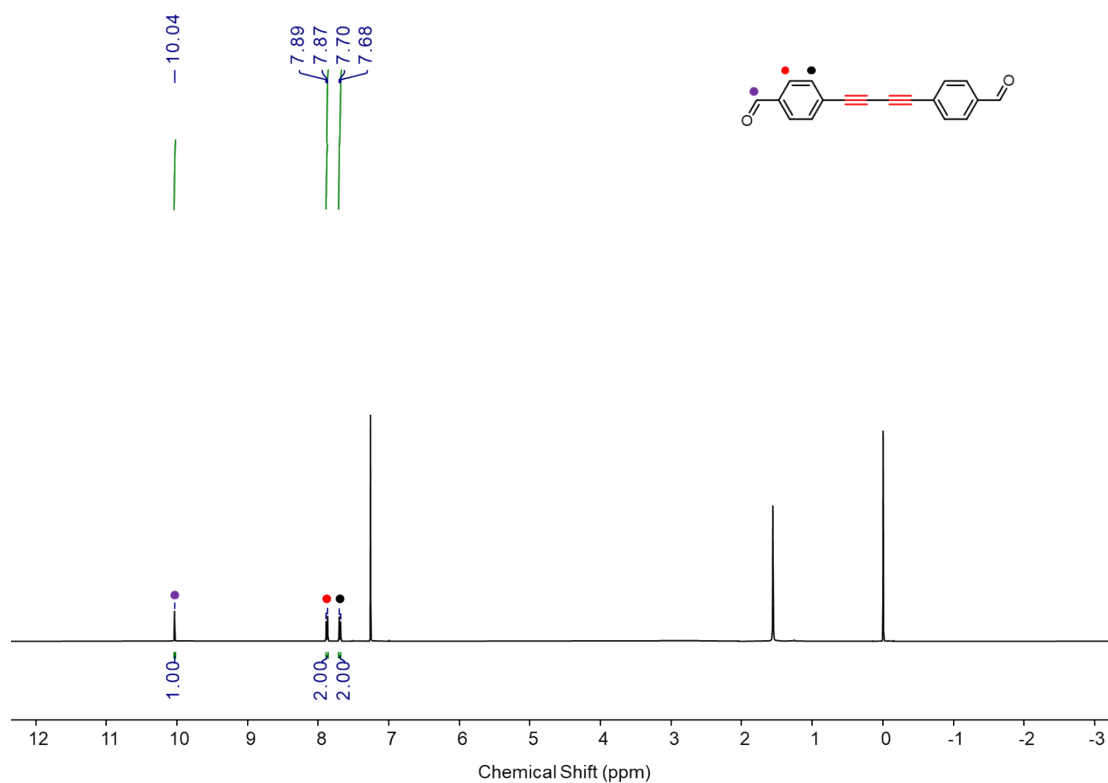
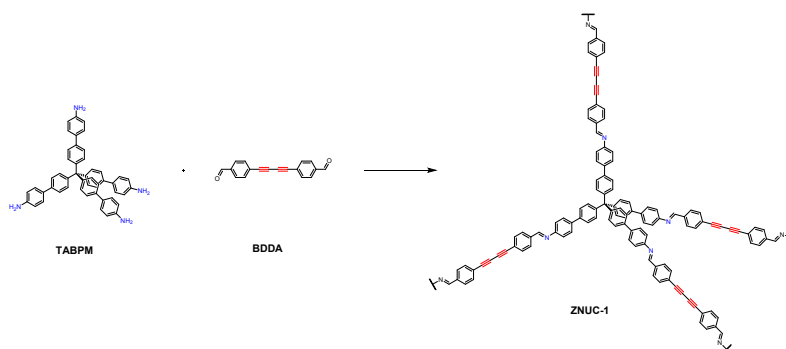


**Fig. S2** The <sup>1</sup>H NMR spectra of 4,4'-(buta-1,3-diyne-1,4-diyl)dibenzaldehyde in CDCl<sub>3</sub>.

## Preparation of ZNUC-1.



A Pyrex tube measuring o.d.  $\times$  i.d. = 10  $\times$  8 mm<sup>2</sup> was charged with tetrakis(4-amino biphenyl)methane (TABPM, 30.8 mg, 0.045 mmol), 4,4'-(buta-1,3-diyne-1,4-diyl)dibenzaldehyde (BDDA, 23.2 mg, 0.090 mmol) in a mixed solution of 1,3,5-trimethylbenzene (1 mL) and 6.0 M acetic acid (0.1 mL). The Pyrex tube was flash frozen in a liquid nitrogen bath sealed under vacuum. Upon warming to room temperature, the tube was placed in an oven at 120 °C for three days. The bright yellow solid was isolated by filtration and washed with THF (3  $\times$  15 mL), acetone (3  $\times$  15 mL) and n-hexane (3  $\times$  15 mL). The powder was dried at 80 °C under vacuum overnight to afford the ZNUC-1 as a bright yellow crystalline solid (36.6 mg, Yield: 70%).

## Synthesis and activation of ZNUC-1-PDA

For example, a 5 mL vial charged with ZNUC-1 (25.0 mg) and diphenyl sulfone (3 g), The vial was then transferred to a tubular furnace and evacuated, filled with N<sub>2</sub> by five cycles. Subsequently, the temperature was raised to 320 °C at the rate of 10 °C min<sup>-1</sup> in a N<sub>2</sub> flowing atmosphere with a flow rate of 20 mL min<sup>-1</sup>. After heating at 320 °C for 3 hours, the temperature was reduced to room temperature at the rate of 10 °C min<sup>-1</sup>. Finally, the obtained product was washed with THF and acetone to remove the residual diphenyl sulfone and dried at 120 °C under vacuum overnight to afford the ZNUC-1-PDA as a dark brown powder.

## Electrical conductivity measurements

Electrochemistry experiments were conducted on a CHI660C Electrochemical Workstation (Shanghai ChenHua Electrochemical Instrument). The obtained powder was ground before being added into a 0.5 cm die. Then, the die pressure was slowly increased to 1.0 MPa and kept for 1 min to prepare pellets (diameter = 0.5 cm, thickness about 0.74 mm). Two pieces of gold (diameter = 0.5 cm) with wires are attached to both sides of the pellet. The current-voltage (I-V) measurement was performed in conditions by sweeping the voltage from -1.0 to 1.0 V. The obtained conductivity was collected at 25 °C in a N<sub>2</sub> atmosphere.

### Section S3. Fourier-transform infrared spectroscopy

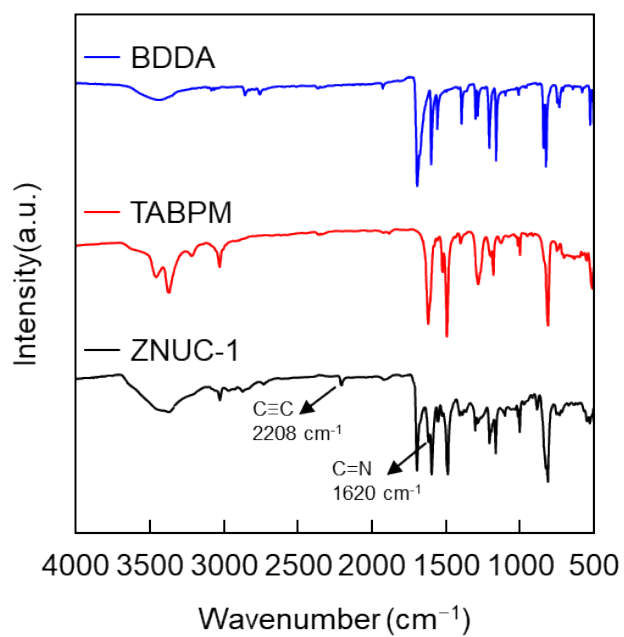


**Fig. S3** FT-IR spectra of BDDA (blue), TABPM (red), ZNUC-1 (black).

#### Section S4. Solid-state $^{13}\text{C}$ NMR spectra

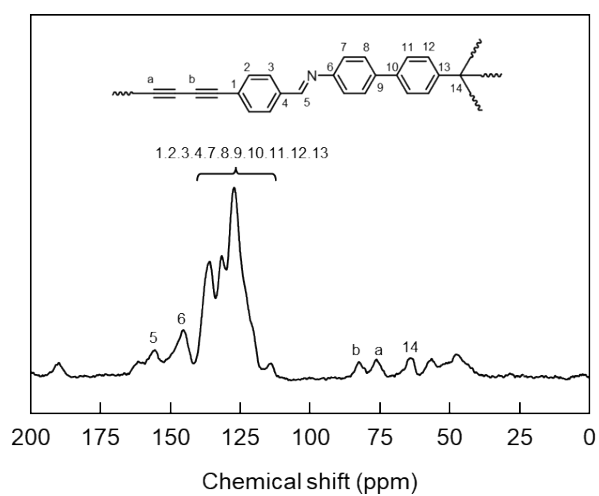


**Fig. S4** Solid-state  $^{13}\text{C}$  NMR of ZNUC-1.

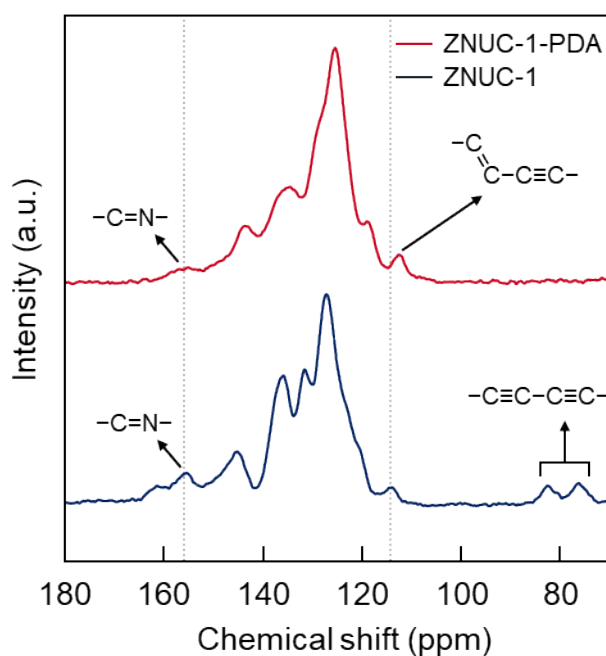


**Fig. S5** Comparison of the  $^{13}\text{C}$  cross-polarization magic angle spinning NMR spectra of ZNUC-1 and ZNUC-1-PDA.

Section S5. SEM image

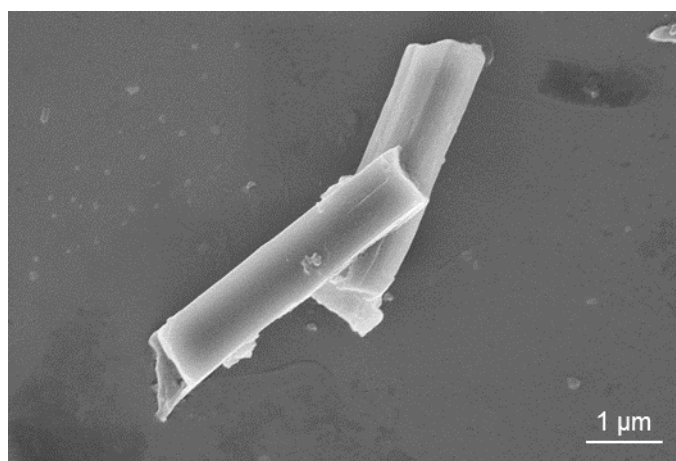


Fig. S6 SEM image of as-synthesized ZNUC-1.

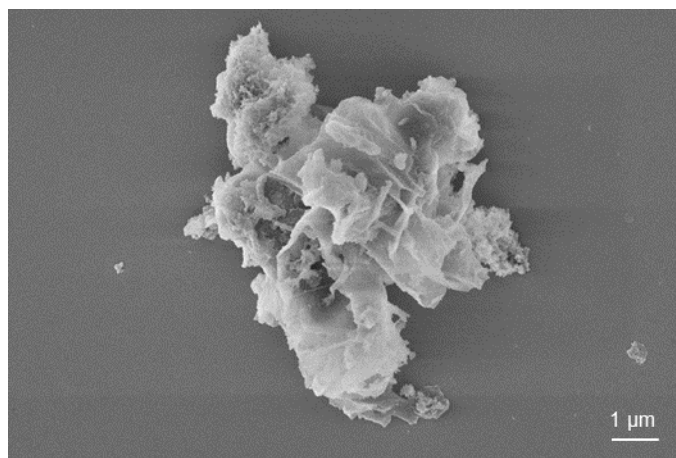
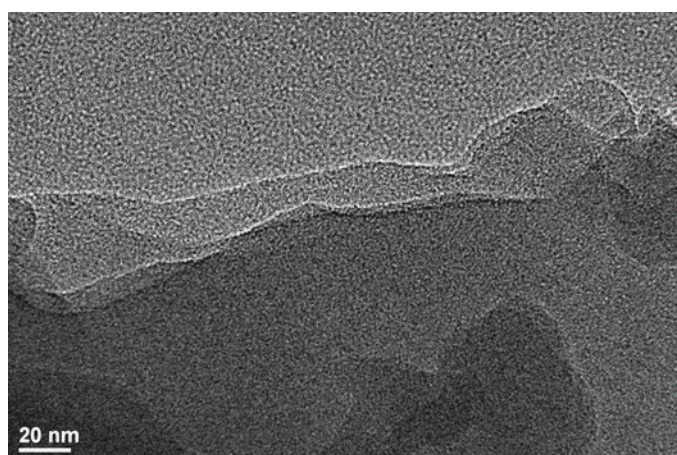
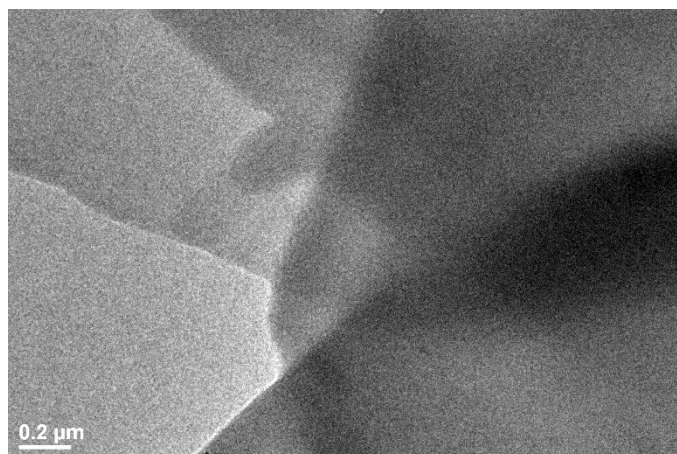


Fig. S7 SEM image of as-synthesized ZNUC-1-PDA.

**Section S6. TEM image**



**Fig. S8** TEM image of as-synthesized ZNUC-1.



**Fig. S9** TEM image of as-synthesized ZNUC-1-PDA.

Section S7. TGA curves

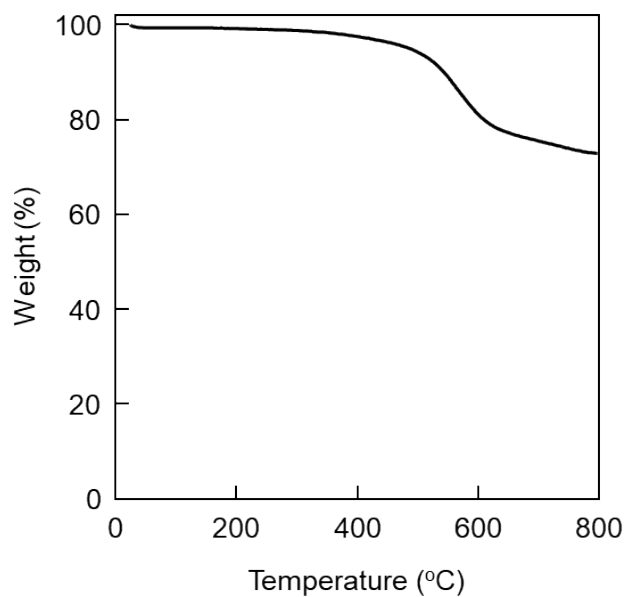


**Fig. S10** TGA curve of ZNUC-1 at the heating rate of  $10\text{ }^{\circ}\text{C min}^{-1}$  to  $800\text{ }^{\circ}\text{C}$  under the  $\text{N}_2$  atmosphere with a  $\text{N}_2$  flow rate of  $10\text{ mL min}^{-1}$ .

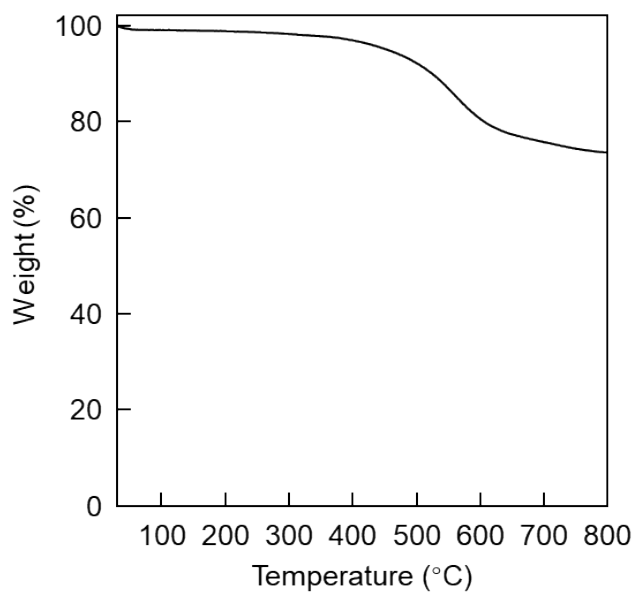


**Fig. S11** TGA curve of ZNUC-1-PDA at the heating rate of  $10\text{ }^{\circ}\text{C min}^{-1}$  to  $800\text{ }^{\circ}\text{C}$  under the  $\text{N}_2$  atmosphere.

## Section S8. PXRD patterns and structures

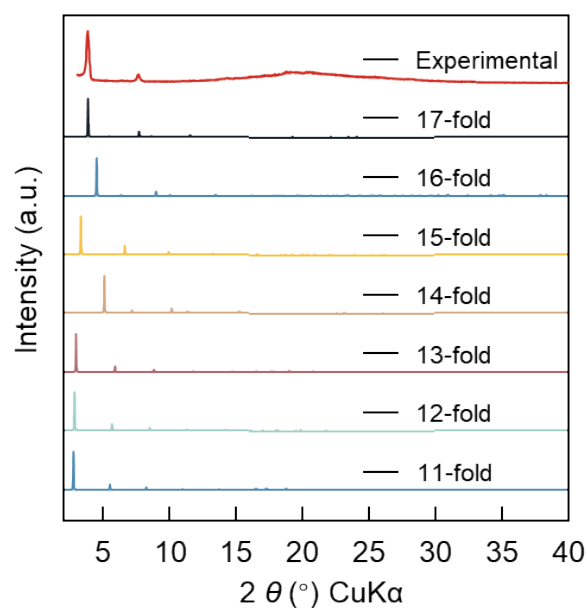


**Fig. S12** Simulated PXRD patterns for possible isomers of ZNUC-1 with different interpenetration degrees from 11 to 17. It can be seen that only the simulated PXRD pattern with 17-fold interpenetrated structure matches with the experimental data well.

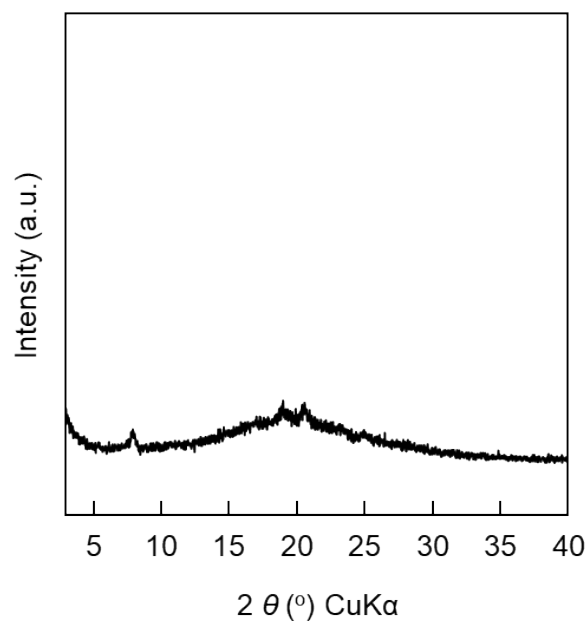


**Fig. S13** PXRD pattern of activated ZNUC-1.

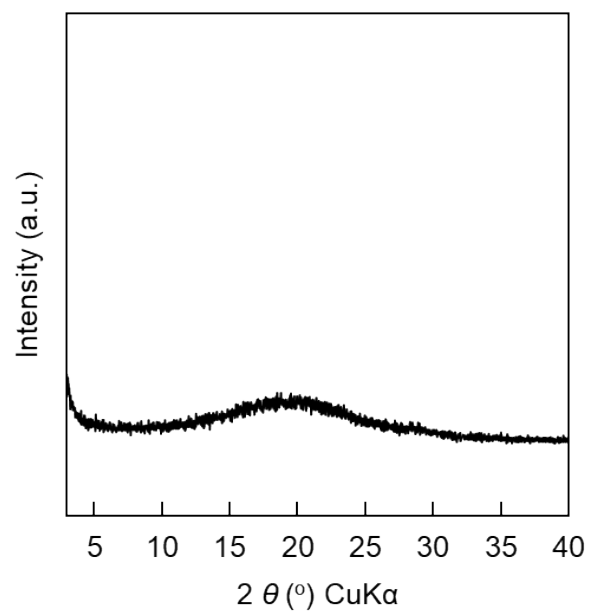


**Fig. S14** PXRD pattern of activated ZNUC-1-PDA.

## Section S9. EDS analysis

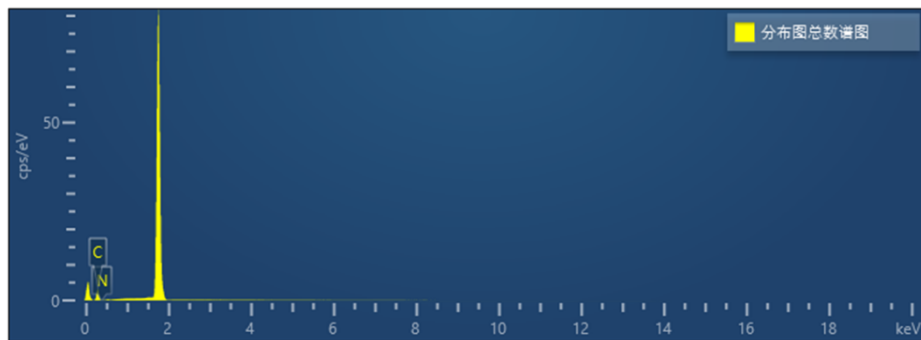


**Fig. S15** EDS elemental content analysis from SEM-related EDS in ZNUC-1-PDA.

## Section S10. Raman spectroscopy analysis

### Acid-digested hydrolysis experiment:

To a flask, activated ZNUC-1-PDA (15 mg), concentrated hydrochloric acid (5.0 mL), and THF (8.0 mL) were added. The mixture was heated under a nitrogen atmosphere at 80 °C for 12 hours. After cooling to room temperature, the insoluble solid was collected by filtration, washed sequentially with deionized water, DMF, acetone, and THF, and then vacuum dried at 80 °C overnight for Raman characterization.

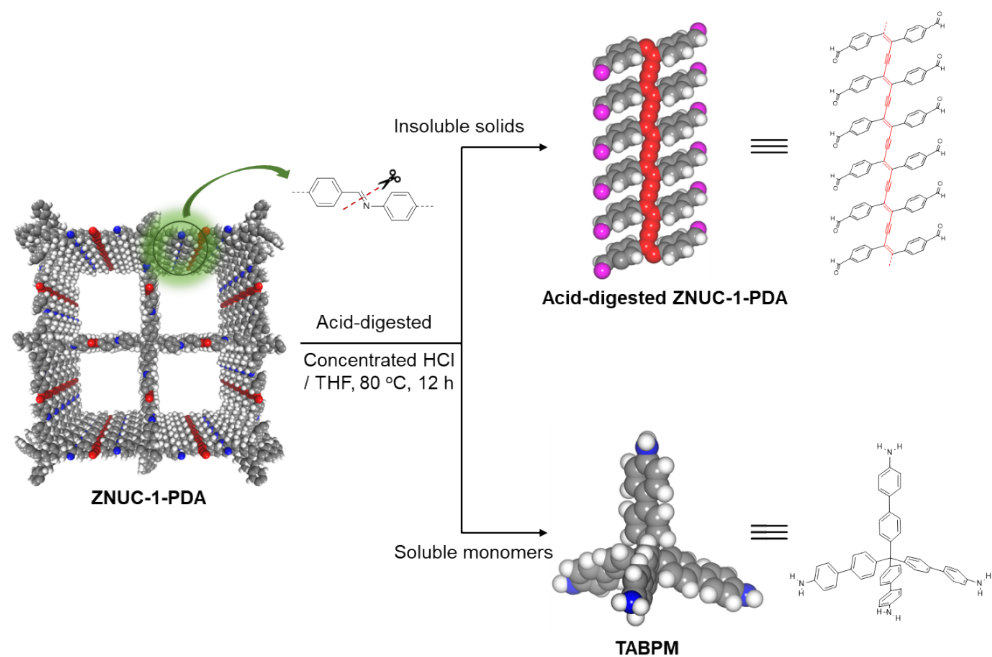


**Fig. S16** Schematic diagram of the acid-digested hydrolysis experiment of ZNUC-1-PDA. The obtained acid-digested ZNUC-1-PDA was used for Raman characterization.

Section S11. UV-visible absorption spectra

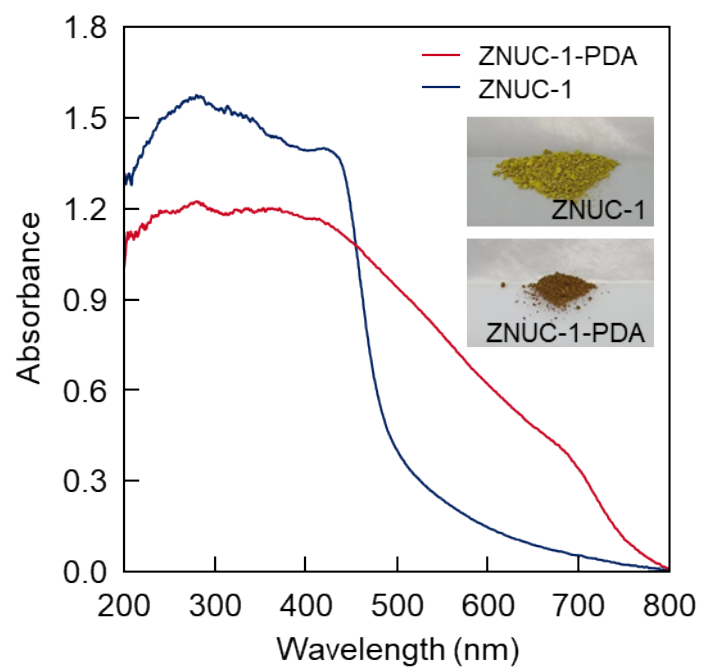


**Fig. S17** UV-visible absorption spectra of ZNUC-1 and ZNUC-1-PDA. Inset: ZNUC-1 (top) and ZNUC-1-PDA (bottom).

## Section S12. Nitrogen adsorption

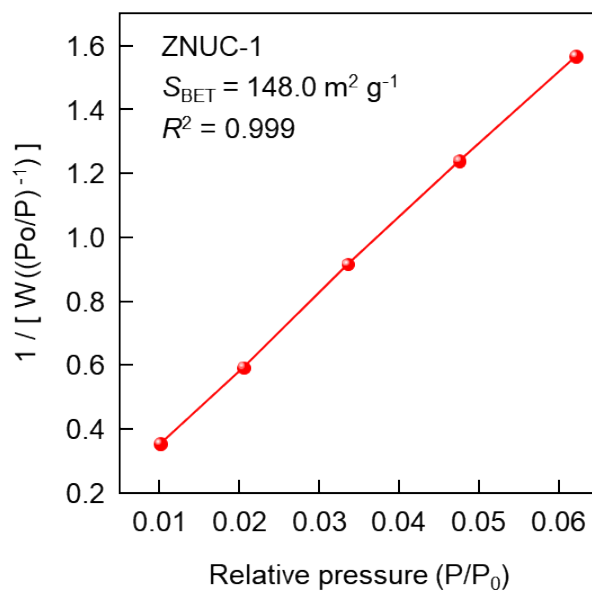


Fig. S18 BET plots of ZNUC-1 calculated from  $\text{N}_2$  adsorption isotherm at 77 K.

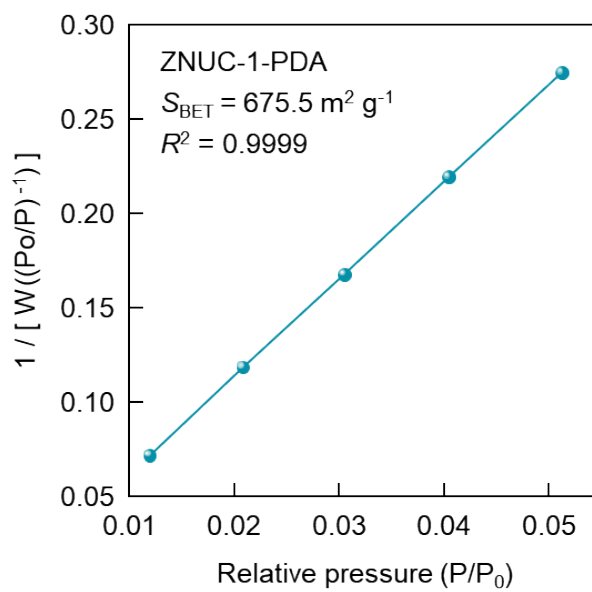
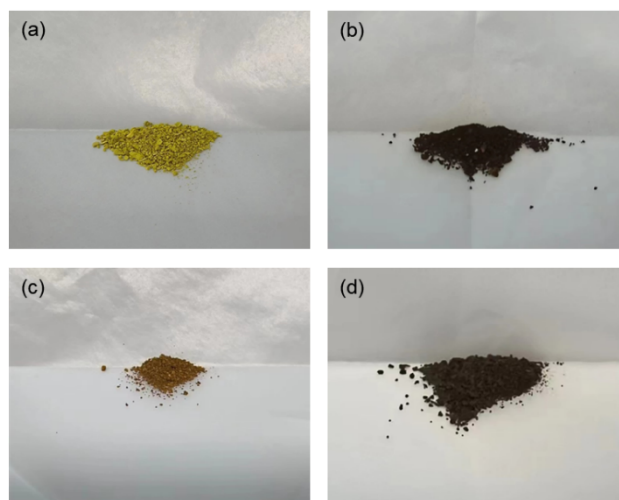


Fig. S19 BET plots of ZNUC-1-PDA calculated from  $\text{N}_2$  adsorption isotherm at 77 K.

### Section S13. Iodine uptake experiments

Vapor-phase iodine uptake measurements were performed by simulating the typical nuclear waste processing.<sup>3</sup> In a typical experiment, about 25 mg of the sample was weighed into a brown vial, and then the vial was loaded into a larger brown vessel containing iodine powder. Afterward, the vessel was sealed and heated at 70 °C in a convection oven. At particular time intervals, the brown vial was removed, cooled to room temperature, and weighed. The uptake capacity was calculated by subtracting the initial mass and dividing the result by the initial mass:  $(m_t - m_0)/m_0$ .



**Fig. S20** The images of the COFs samples before (a: ZNUC-1, c: ZNUC-1-PDA) and after (b: I<sub>2</sub>@ZNUC-1, d: I<sub>2</sub>@ZNUC-1-PDA) the vapor phase iodine uptake.

## Section S14. Electrical conductivity measurements

The electrical conductivity of the samples was evaluated through I-V characteristic testing using a two-probe configuration with gold paste contacts.

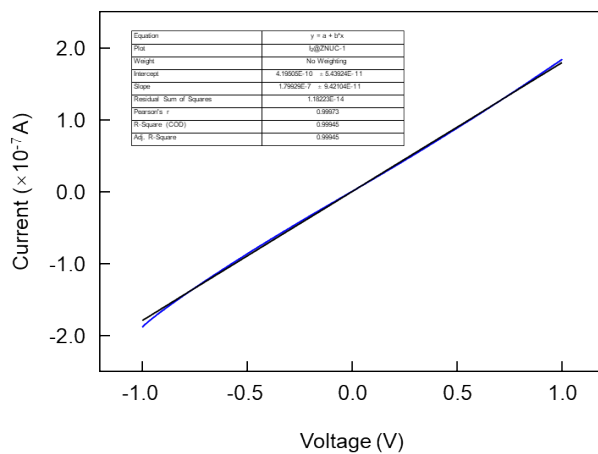


Fig. S21 I-V curves of I<sub>2</sub>@ZNUC-1.

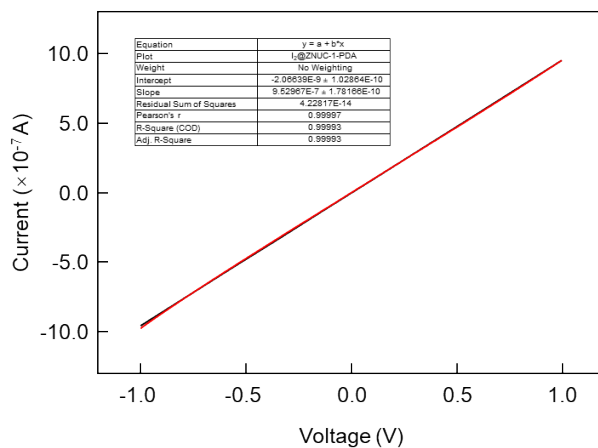


Fig. S22 I-V curves of I<sub>2</sub>@ZNUC-1-PDA.

## Section S15. Fractional atomic coordinates

**Table S1.** Unit cell parameters and fractional atomic coordinates of ZNUC-1.

Space group	$I4_1/a$ (No. 88)		
Calculated unit cell	$a = b = 45.9820 \text{ \AA}, c = 6.7346 \text{ \AA},$ $\alpha = \beta = \gamma = 90^\circ$		
Measured unit cell	$a = b = 45.9680 \text{ \AA}, c = 6.7124 \text{ \AA},$ $\alpha = \beta = \gamma = 90^\circ$		
Pawley refinement	$R_p = 3.46\%, R_{wp} = 4.44\%$		
Atoms	x	y	z
C	0.03162	0.52211	1.02284
C	0.05584	0.52274	1.14739
C	0.07555	0.49954	1.15160
C	0.07112	0.47613	1.02189
C	0.04687	0.47544	0.89651
C	0.02696	0.49895	0.88958
C	0.10326	0.47272	1.41498
C	0.12168	0.47264	1.57984
C	0.13560	0.49814	1.64138
C	0.13191	0.52368	1.52848
C	0.11341	0.52380	1.36368
C	0.09839	0.49848	1.30757
C	0.16333	0.51910	1.91657
N	0.15285	0.49704	1.81940
C	0.18437	0.48691	2.18258
C	0.20021	0.48348	2.35835
C	0.21208	0.50777	2.45383
C	0.20811	0.53551	2.37282
C	0.19227	0.53898	2.19728
C	0.18026	0.51475	2.10050
C	0.24200	0.50157	2.78630
C	0.22835	0.50431	2.63477
H	0.01509	0.54058	1.02758
H	0.05981	0.54233	1.24758
H	0.08735	0.45740	1.01785
H	0.04286	0.45574	0.79754
H	0.09203	0.45179	1.36653
H	0.12552	0.45163	1.66582
H	0.14403	0.54437	1.57136
H	0.11041	0.54456	1.27343
H	0.15931	0.54201	1.85813
H	0.17472	0.46709	2.10511
H	0.20347	0.46087	2.42412
H	0.21780	0.55533	2.45001

H	0.18903	0.56161	2.13174
C	0.00000	0.50000	0.75000

---

## Section S16. References

- 1 Z. Li, L. Sheng, C. Hsueh, X. Wang, H. Cui, H. Gao, Y. Wu, J. Wang, Y. Tang, H. Xu, and X. He, *Chem. Mater.*, 2021, **33**, 9618-9623.
- 2 M. Wierzbicka, I. Bylinska, A. Sikorski, C. Czaplowski and W. Wiczak, *Photochem. Photobiol. Sci.*, 2015, **14**, 2251-2260.
- 3 S. Walker, R. A. Hyde, R. B. Piper and Roy, M. W. An overview of in situ waste treatment technologies. Spectrum 92: nuclear and hazardous waste management international topical meeting, Boise, ID, Aug 23-27, 1992; American Nuclear Society, 1992; p 12.